J Solid State Electrochem (2005) 9: 121–131
DOI 10.1007/s10008-004-0523-z

ORIGINAL PAPER

Shou-Shing Hsieh · Ching-Fang Huang · Jenn-Kun Kuo
Huang-Hsiu Tsai · Sheng-Huang Yang

SU-8 flow field plates for a micro PEMFC

Received: 7 January 2004 / Accepted: 25 February 2004 / Published online: 26 January 2005

Abstract A SU-8 photoresist microfabrication process was developed for micro proton exchange membrane fuel cell flow structures for both anode and cathode flow field plates with a cross section of 5 cm^2 (22.5 mm×22.5 mm) and thickness (for a single cell) of about 750 μm. The new design for flow field plates would have SU-8 used as not only a photoresist but also as a microstructure material. A thickness of 30 nm Pt sputter loading deposited onto a Nafion 117 for membrane electrode assembly was made, with both scanning electron microscopy and atomic force microscopy characterization. Air flows were completed in hydrogen fuel cells with air breathing and forced air flows of low input pressure as well as low velocity. Performance tests of polarization curves and power density distribution as well as impendence measurements were conducted and discussed to examine the effects of orientation of the cathode surface with five hydrogen feeding rates as well as different airflow feeding modes.

Keywords SU-8 flow field plates · Microfabrication · Micro proton exchange membrane fuel cell · Cell performance

Introduction

Consumers now have available to them a wide and increasing spectrum of portable electronic telecommunication and computer devices, including cellular phones and laptop computers. Due to such rapidly growing portable electronics markets and the needs for other applications, for instance, game devices and music systems, more advanced and more miniaturized portable devices to overcome the systematic limitations of conventional rechargeable batteries are in demand. The proton exchange membrane fuel cell (PEMFC) has the potential to meet these requirements [1, 2].

Miniaturizing fuel cells for portable applications, as mentioned for computer, communication and consumer products, however, is not simply a matter of reducing the corresponding components' dimensions. Rather, new design and manufacturing processes must be examined and developed simultaneously.

Traditional/conventional macro-sized fuel cell components are limited by characteristic fabrication constraints, such as the constraint on the machining of flow passage by the brittleness of graphite, and molding being limited in deep narrow channels. The traditional processes of cutting, drilling, molding, grinding, etc. will become less economically viable while dealing with a rather small PEMFC. Instead, processes such as fabrication methodologies used in the conventional semiconductor industry may be more appropriate in batch, as well as continuous production to manufacture a micro fuel cell to reach a powerful, highly efficient and low cost goal.

To meet the low cost goal, several previous investigators have recently extensively examined the sputter deposition technique by using ultra-low levels of catalyst loading [3] and it has been proven to be a cost-competitive technology [4, 5]. In addition to membrane electrode assemblies (MEAs), to decrease the current resistance of the cell components, integrated flow field channels with current collectors were designed and microfabricated. This technique was reported in [5]. To ease fabrication processes and facilitate future mass production, a novel microstructure and material is thus proposed.

Although much work has been done on single cells of PEMFC or their components such as membrane electrolytes, catalysts and structure, electrochemical reaction mechanisms and kinetics, electrode materials and preparation [6], as well as H_2 and air feeding conditions

S.-S. Hsieh (✉) · C.-F. Huang · J.-K. Kuo
H.-H. Tsai · S.-H. Yang
Department of Mechanical and Electro-Mechanical Engineering, National Sun Yat-Sen University, Kaohsiung, Taiwan, ROC
E-mail: sshsieh@mail.nsysu.edu.tw
Tel.: +886-7-525-2000
Fax: +886-7-525-4215

[7], there are only a few studies on micro PEMFC. In fact, as mentioned in [1], the design concepts and considerations for miniaturized PEMFCs are essentially different from those of PEMFCs. Consequently, it is necessary to re-examine the influences on cell performances for the major parameters such as hydrogen and air streams feeding rates as well as feeding conditions and the orientation of the cathode surface.

Based on the foregoing discussion, SU-8 processes will be implemented with the present deep UV lithography microfabrication of a micro PEMFC. The present SU-8 is not only a photoresist material but functions as a microstructure for flow channels. The study is a continuation of the authors' previous work [5] to further examine operating performance of a LIGA-like microfabrication process with Pt sputter-loaded MEAs and SU-8-built flow field passages for a micro PEMFC.

Fuel cell design

A PEMFC typically consists of a membrane, two electrodes, two current collectors and two sets of flow channels. Instead of the three components of the conventional fuel cell, electrode, current collector and flow field plate, the present integrated design as reported in [5] would make these three components in one. There is no carbon paper for the present micro fuel cell design. Based on this design concept, the present micro PEMFC would consist of two sets of SU-8 flow field plates of thickness 200 μm and width 200 μm made by a LIGA-like deep UV lithography, and integrated with a thin (~50 μm) copper foil and an ultra thin Pt sputtering deposited (~30 nm) on a Nafion 117 membrane. Since the ribs between the flow channels do not contact with reactants at all and, in addition, the electric conductivity of the catalyst layer is usually very low, the very thin Ag film, sputtered as mentioned before, can lead electric current to the ribs, thereby improving the overall electric conductivity. MEAs preparations were followed by O'Hayre et al. [4] and Hsieh et al. [5]. As a result, a thin film Pt MEA was used. It consisted only of ultra-thin sputtered Pt films deposited directly onto Nafion 117 (183 μm) membranes (ElectroChem) via a PRG 300RF sputter. Related Nafion membrane cleaning processes before sputtering and the sputter operating conditions are also similar to Hsieh et al. [5]. Detailed geometric design and fabrication parameters are listed in Table 1. The advantages of the present design and integrated microfabrication are as follows:

-1. A few nanometers (~30 nm) sputtered Pt film corresponding to a catalyst loading level of 0.12 mg/cm^2 can be reached.
-2. The material SU-8 used for the flow field plate is light and cost-competitive, especially for mass production [8].
-3. Ag sputtered loading (~0.2 μm) deposited on the top of the rib between the flow channels, bottom and lateral side walls of the flow channel used as a current collector would improve the electrical conductivity performance.

Overall, for this single micro PEMFC, two sets of flow field plates (~250 μm each), a Nafion 117 membrane with about 180 μm thickness, and two Pt catalyst layers of about 30 nm each are required, giving a single cell thickness of about 750 μm.

Table 1 Geometric design and fabrication parameters. *PR* Photoresist

PR coating	SU-8 100
PR property	Negative
PR type	Thick film
Speed (rpm)	1000
Soft bake at 95 °C (min)	30
UV light wave length (nm)	365
Light intensity (mW/cm^2)	40
Exposure time (s)	24
Hard bake at 95 °C (min)	2
Development (min)	3

SU-8 micro-structured flow field plates

In addition to reducing the thickness of the flow channels, micro-structured flow field plates are gas-tight and have high electrical conductivity. Instead of diffusion processes going by traditional carbon paper or cloth, convective transport phenomena between reactants and electrodes would occur, which would greatly improve the cell performance.

A LIGA-like microfabrication process of deep UV lithography with SU-8 thick photoresist material was used to fabricate the microchannels for flow fields. It is described in detail below and illustrated in Fig. 1.

-1. The substrate, a 50 μm-thick Cu film was cleaned with acetone for 3 min and heated to 150 °C for 3 min for dryness.
-2. Spin coating of SU-8 to a thickness 200 μm was carried out; different rotating speeds (500 rpm for 120 s, 1000 rpm for 60 s, and 500 rpm again for 5 s) were applied to the Cu substrate.
-3. Soft baking for about 35 min was applied (50 °C for 5 min, 90 °C for another 5 min, and 95 °C for 25 min).
-4. Ultraviolet light with a wavelength at 350 nm was used for the exposure process; SU-8 was lithographically structured simultaneously.
-5. Once exposure was completed, heat was applied again for a post-exposure bake of about 8 min.
-6. Development was done with an ultrasonic wave oscillator for a microstructured channel (200 μm depth, 200 μm width with a 50 μm rib).
-7. Ag film (0.2 μm) was sputtered onto the top of the ribs between the channels and lateral side walls and bottom floor of the channels.

One of the resultant channels is shown in Fig. 2a and b, respectively for channel corner and middle regions.

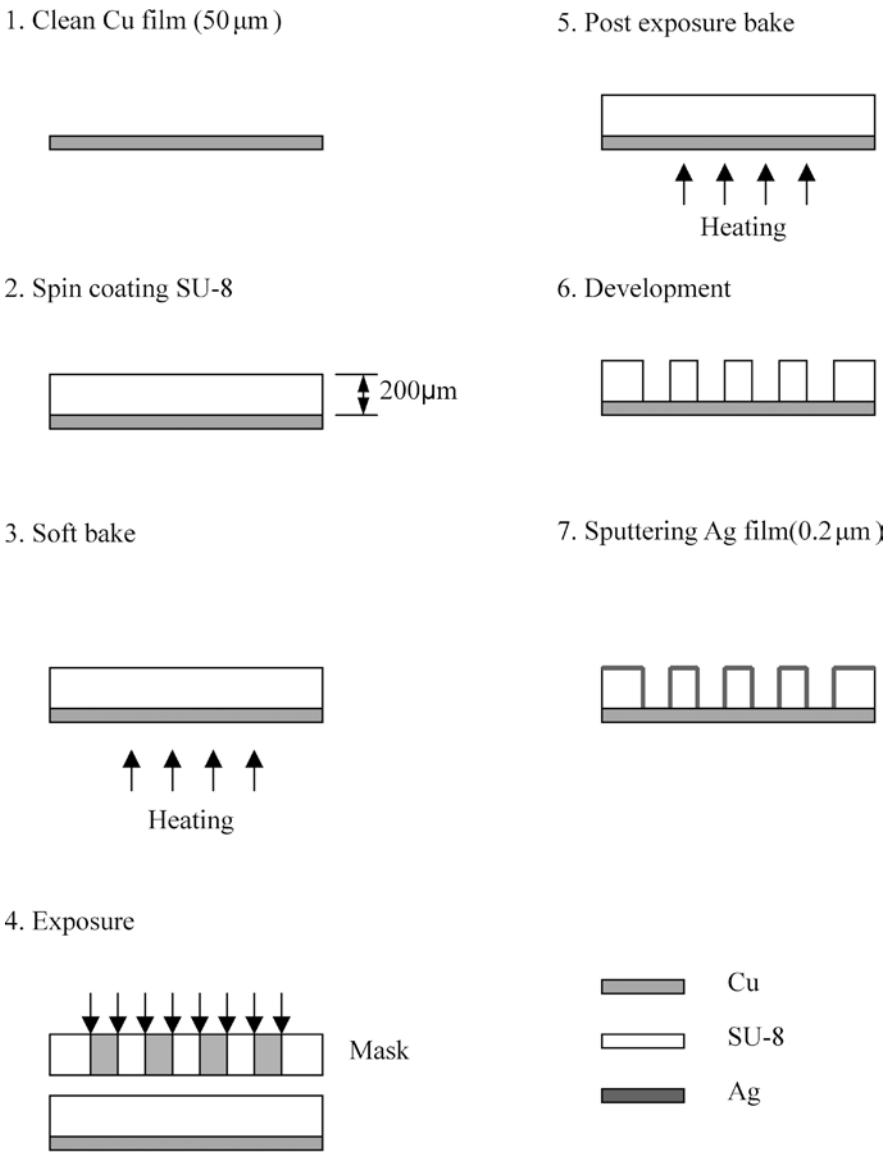

Fig. 1 Fabrication processes of flow field plates

The silvered-sputtering channel is shown in Fig. 3a, and the final assembled single fuel cell is shown in Fig. 3b. During the assembly, a surface mount technology (SMT), UV curing, was used for these Su-8 flow channels with MEAs.

Materials and methods

MEA preparation To minimize the weight of the fuel cell, thin film Pt MEAs were used [4, 5]. They consisted of only ultra-thin sputtered Pt films deposited directly onto Nafion membranes. With such a design, there would be no any other material added/used in their construction. The deposited Pt thickness was controlled by the sputtering time. Sputter conditions were 80 W and 50 sccm Ar, resulting in a sputter deposition rate of approximately 0.5 nm/s. Sputtered MEA samples were thus prepared with nominal Pt film thicknesses ranging from 30 to 60 nm.

Cell polarization measurements and electrochemical impedance spectroscopy All fuel cell polarization measurements were conducted at room temperature (~25 °C) using dry hydrogen and air at 1 atm pressure. Hydrogen gas flow rates were regulated at 6, 7, 8, 9 and 10 sccm, and measurements were conducted through a Gamry PC 4/750 potentiostat linked to an IBM PC. Electrochemical impedance spectra (EIS) were also measured under the same cell polarization measurement conditions.

Voltage versus current (VI) and power density versus current (PI) curves as well as EIS were measured under different orientations of the cathode surface and dry hydrogen feed rates to examine their effects on the fuel cell performance. The test conditions are shown in Table 2. Pure hydrogen (99.999% H_2) and air (forced and air breathing) were used for the reactant gases on anode and cathode sides, respectively. Five H_2 feeding rates (6, 7, 8, 9, and 10 sccm) were used. A mini fan was installed at top of the air channels to blow air flows to

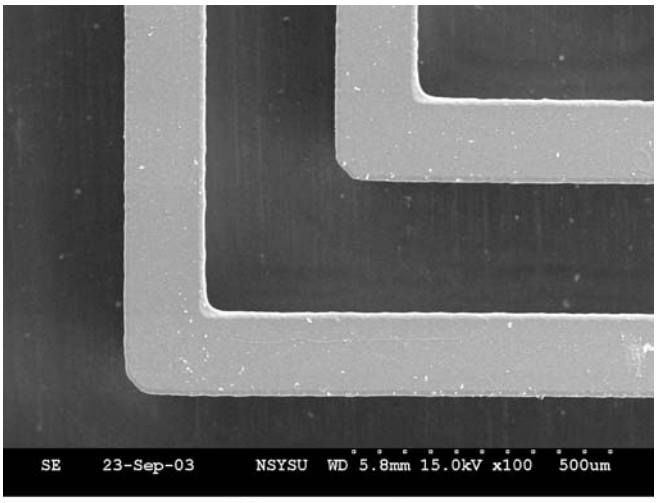

(a) corner region

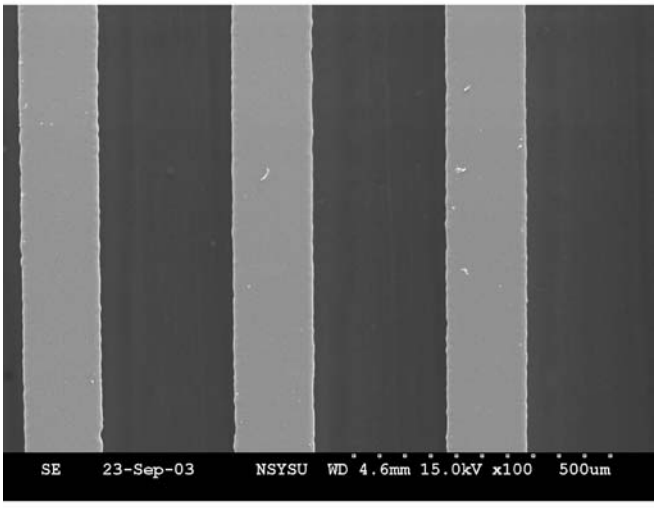

(b) top channel

Fig. 2a, b Photographs of micro flow field channel (200 μm× 200 μm)

the channels, with a resulting inlet velocity of about 25 cm/s.

EIS as specified were measured under the same cell polarization conditions over the frequency range 1 mHz–60 kHz. A small sinusoidal excitation at 10 mV potentiostatic signal amplitude was used and a full cell impedance was measured throughout the present experiments.

Scanning electron and atomic force microscopies The resultant sputtered MEAs were subjected to cross-sectional view scanning electron microscopy (SEM) and atomic force microscopy (AFM) imaging to verify the sputter-deposited film thickness and top-view SEM and AFM imaging to determine surface characteristics and morphological conditions. Both studies were performed in an air clean room under normal atmospheric conditions using Model JSM 6330TF, JEOL and EX 139710, TOPMETRIX for SEM and AFM, respectively.

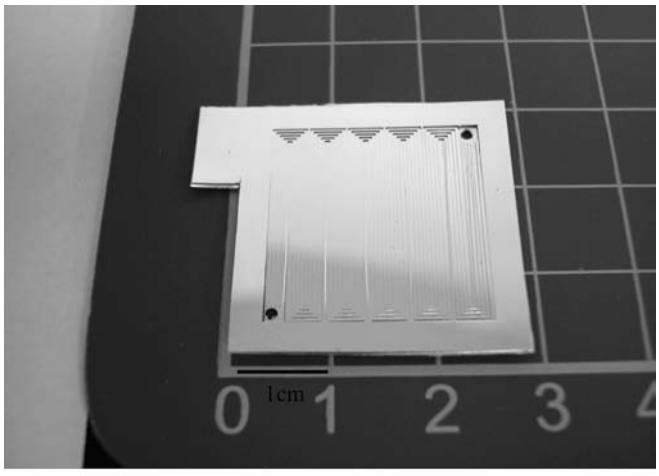

(a) Flow field plate with thin Ag film

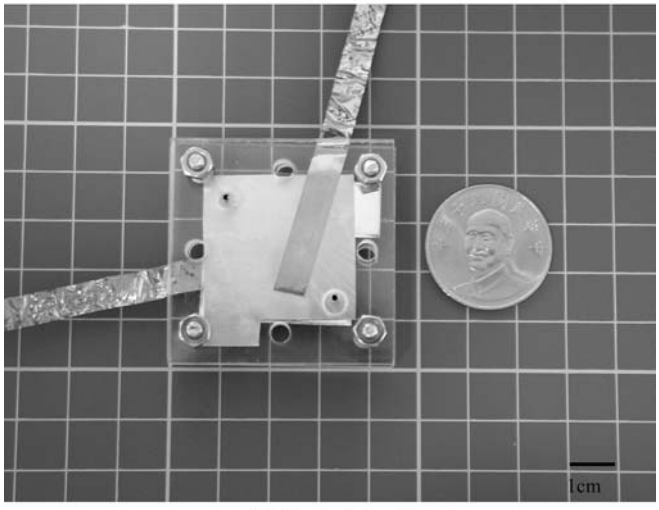

(b) Single fuel cell

Fig. 3a, b Photographs of micro fuel cell

Results and discussion

Microscopy investigation of sputtered Pt

The top-view SEM image in Fig. 4a was analyzed to determine the surface coverages of the sputter-deposited Pt films. Generally, Pt was deposited as a continuous film on the Nafion 117 substrate with few cracks. This is

Table 2 Fuel cell test conditions

Cell operating temperature (°C)	25
Pressure (atm)	2.72 (anode) 1 (cathode)
Channel size (μm)	200 (depth) 200 (width) 100 (rib)
Feed stream (sccm)	Anode: hydrogen 6, 7, 8, 9 and 10 Cathode: air breathing and forced air

consistent with O'Hayre et al. [4] and Hsieh et al. [5]. The cracks were relatively fine, about 0.05 μm wide (Fig. 4a), and spaced on average 10–15 μm (Fig. 4a) apart. The surface coverages were used in conjunction with the film thickness from the corresponding cross-sectional SEM image (see Fig. 4b) to calculate the subsequent Pt loadings (about 0.12 mg/cm^2). The cross-sectional view in Fig. 4b shows that a thickness of 30 nm of Pt was secured. Additional optical microscope imaging of the above is given in Fig. 5. Here a zoomed out perspective of a square area 200 nm×200 nm with 3-D topography is shown in Fig. 5a and Fig. 5b, respectively. The surface coverages indicate the morphological conditions. Significant surface texturing was found as evidenced by Fig. 5b.

Effect of orientation of the cathode surface

For airbreathing (i.e., free convection mode), three different installations of the cathode surface were made, namely, vertical, horizontal and 45°-oriented. The output potential and power density versus the current density are shown in Fig. 6a, b, i.e., VI and PI curves. It is known that the cell polarization curve is generally composed of three stages, which are concerned with the activation losses, the ohmic losses and the mass transport losses when the cell is operated at a low temperature, as in the present study. However, it seems that the present cell polarization under H_2/air does not have three stages but only two, i.e., there was no rapid initial fall due to the sluggish kinetics of

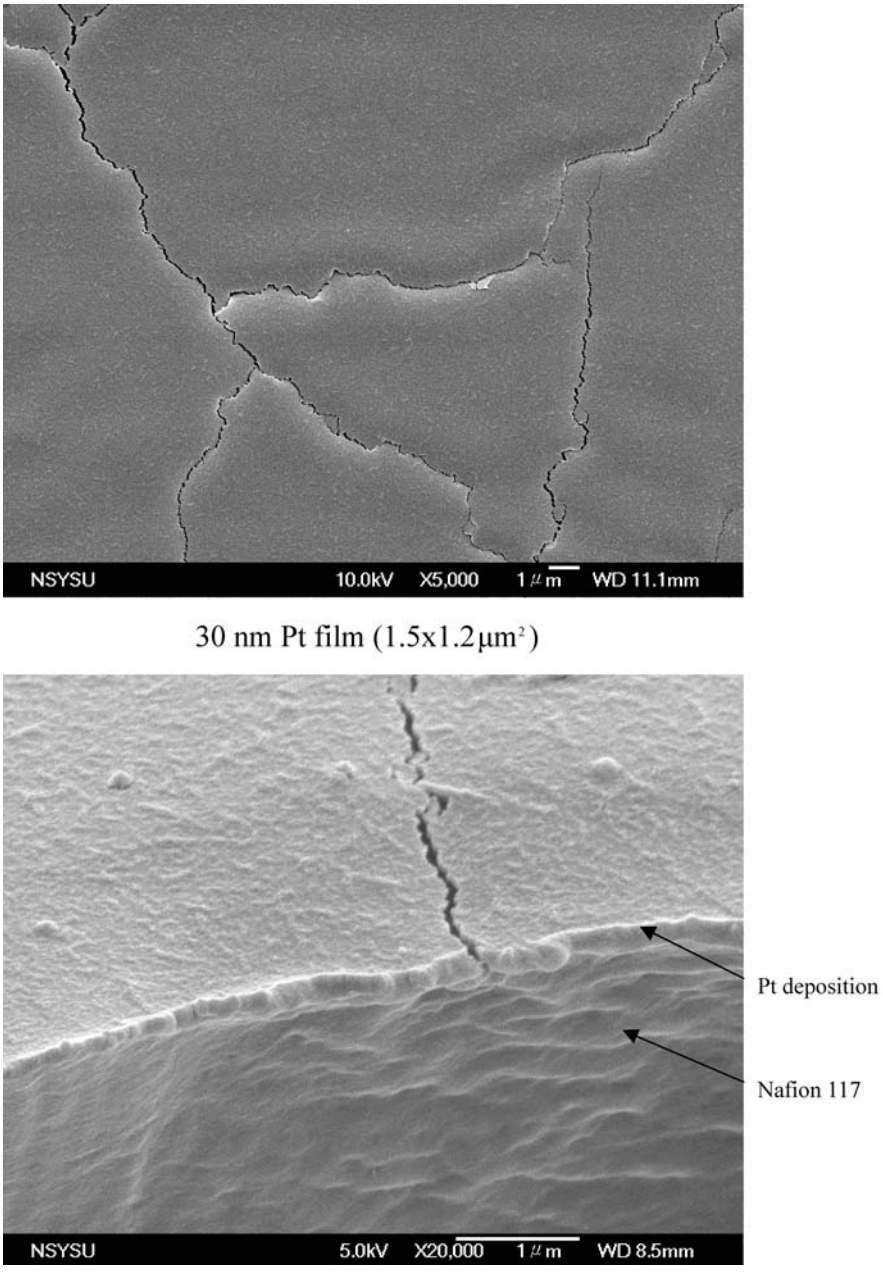

Fig. 4 Scanning electron microscopy images showing the morphological evolution of thin Pt film sputtered on Nafion 117

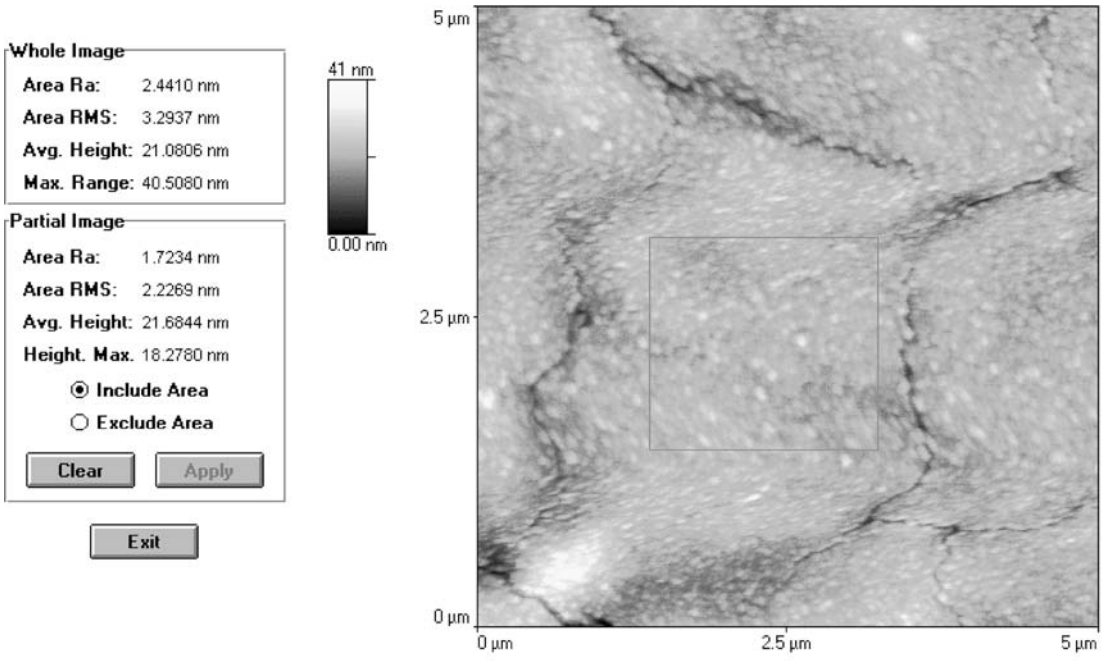

(a) Top view (200 nm×200 nm)

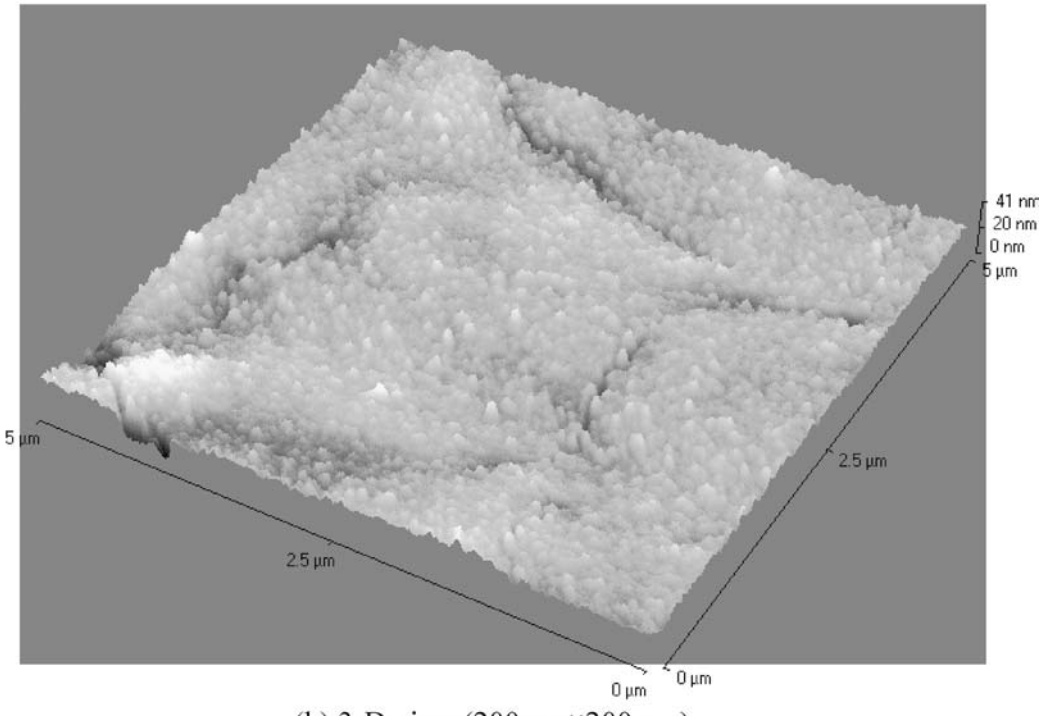

(b) 3-D view (200 nm×200 nm)

Fig. 5a, b Atomic force microscopy images showing the morpho-

oxygen reduction at cathode. The curves shown in Fig. 6a have a common trend. It was found that the cathode surface inclined 45° from the vertical position would have a slightly better cell performance, followed by the horizontal and vertical installations. Making a close-up examination of Fig. 6a, b, such differences in cell voltage and power density are small compared to the conventional PEMFCs results from [7] with the same orientations. This is mainly due to the miniaturized nature of the micro fuel cells. For example, the ratio of surface area to the volume of a micro fuel cell is large which results in ''orientation-free'' results.

Effect of hydrogen feeding rates on fuel cell performance

The effect of hydrogen feeding rates (6, 7, 8, 9, and 10 sccm) with 45° orientation of the cathode surface on the cell performance of the present single cell is shown for VI curves and power density, respectively, in Fig. 7a and b. Figure 7a represents the results of potential-current correlations. For all the tests of this study, as stated before, the VI curves have an initial very modest voltage drop at a very small current range, differing from those in conventional fuel cells which have a rapid initial fall due to electrochemical activation processes, followed by the ohmic polarization phenomenon, where a nearly linear potential drop with an increase of current density occurs. Finally, as current density increases to a certain value ($\geqq 60$ mA/cm^2), a mass-transport limitation phenomenon takes place with an exponential fall. The exact reasons for this are still not understood. It is perhaps due to the characteristics and nature of a micro PEMFC.

Among these five hydrogen feeding rates, it was found that the fuel cell performance had the highest value at 8 sccm (Fig. 7a). This is also shown in Fig. 7b

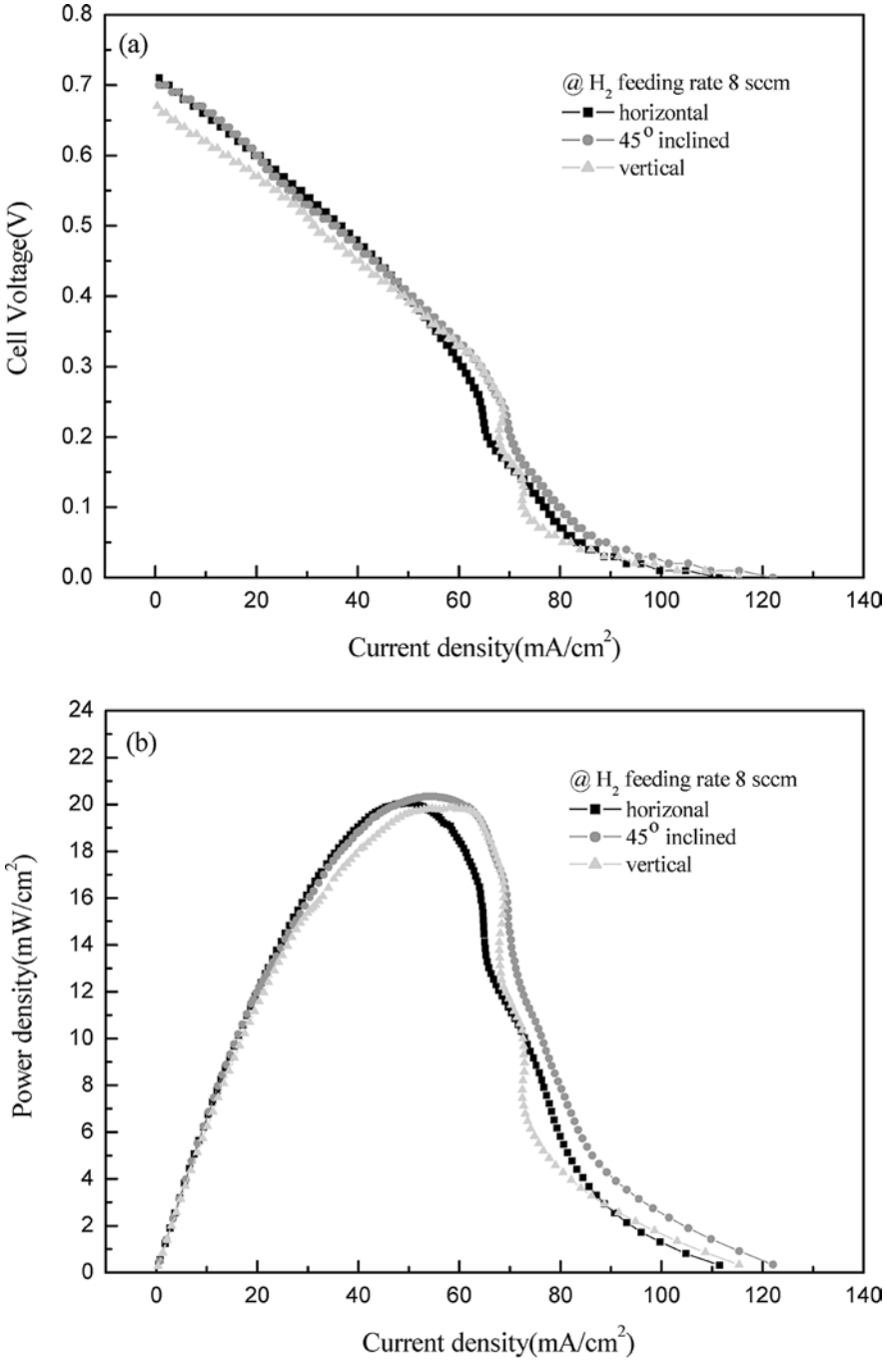

Fig. 6a, b Micro proton exchange membrane fuel cell (PEMFC) performance test at different orientations

from the corresponding power density-current curves. Basically, an increase in H_2 feeding rates would result in a relative increase in fuel cell performance; however, we seem to have found an optimum increase in the present study: H_2 feeding rates at 8 sccm produce the best performance as far as VI and PI curves are concerned.

The reasons for the above findings are based on two counterbalancing factors occurring in the above processes. An increase of H_2 rates would increase the number of protons that move to the cathode through the membrane, which enhances the cell performance; however, in the meantime, the ionic conductivity of the membrane is limited due to the mass-transport limitation on the cathode. Such ''choke and traffic jam'' effect on the membrane and at the cathode would deteriorate the cell performance even though the ionic conduction and the reaction processes at the cathode are separated. However, we have to admit the entire reaction is continuous; one factor would influence the other.

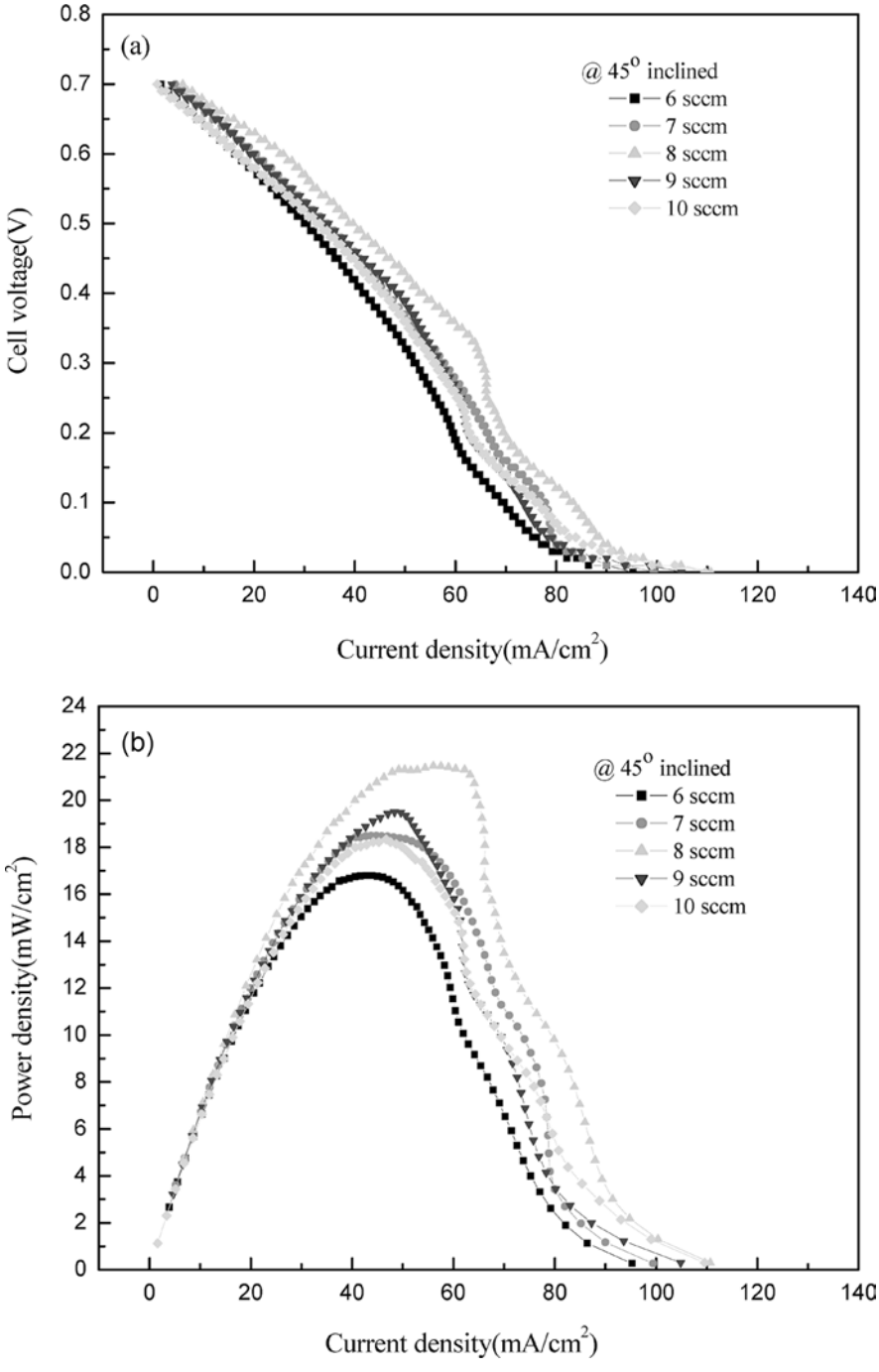

Fig. 7a, b Micro PEMFC performance at different H_2 feeding rates

Effect of airbreathing (free convection) and forced airflows

The presented results for a micro fuel cell do show different trends for air breathing and forced airflows. Fig. 8a, b show VI and PI distribution at 45° orientation of the cathode surface for a forced airflow with three different H_2 feeding rates.

The results indicate that with forced air the best cell performance takes place at an H_2 feed rate of 10 sccm, which is different from the previous findings (Fig. 7a, b). Much more H_2 gas was needed to warrant the minimum electrochemical reaction taking place as the forced air was used in the cathode. This is because at this stage, the amount of reactant gas that reaches the three-phase zone where the reaction takes place increases. In addition, the cell performance of VI and PI shows higher values than those of airbreathing (i.e., free convection mode). For forced air, the current density can reach 140 mA/cm^2 and power density is up to 29 mW/cm^2 at 80 mA/cm^2, while, for airbreathing, it is about 22 mW/cm^2 at a current density of 60 mA/cm^2 with a maximum current density of about 120 mA/cm^2. Based on the above re-

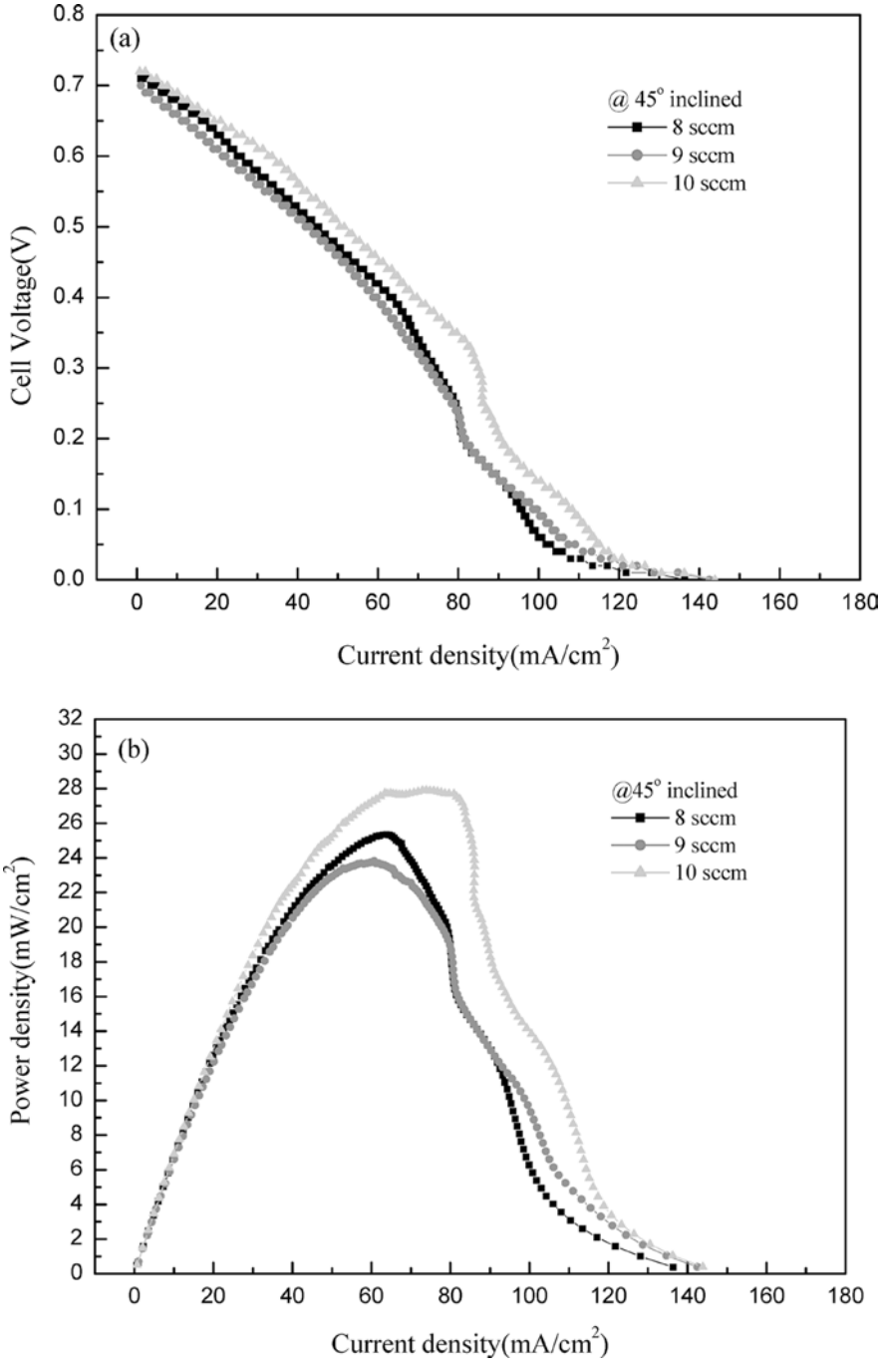

Fig. 8a, b Micro PEMFC performance test on cathode forced convection

sults, the forced air is essential while one operates such a micro PEMFC at room temperature.

EIS examination

When the impedance of a full cell was measured, the impedance spectra revealed information about both cathode and anode impedance. In fact, the anode impedance was nearly equal to the cathode impedance due to a fast hydrogen oxidation reaction at the anode. Figure 9 shows a typical impedance spectra of a H_2/air single cell with three feeding rates at a voltage of 0.6 V for a 45°-inclined cathode surface. Among the three flow rates, the high frequency and medium frequency arcs seem unchanged for 6 and 8 sccm flow rates; however, a small change occurs at 10 sccm. In fact, at the low frequency (<100 Hz), there seems no change in Fig. 9. This can be further examined in Fig. 10 as well. This indicates that at low frequency the effect of mass transfer of O_2 is the same, while the high frequency arc is for activation kinetics of O_2. In fact, oxygen kinetics and oxygen diffusion are two factors that limit the performance of the cell. Generally, the semi-circle size is determined by the size of the low frequency arc and the diameter of the semi-circle, which corresponds to the polarization resistance. The polarization resistance is a combination of charge transfer resistance and gas diffusion resistance. As the current density increases, the gas diffusion resistance becomes more dominant than the charge transfer resistance. This indicates that the polarization resistance becomes mass-transfer controlled.

Although the present impedance spectra arc is not closed, the polarization resistance can still be found from a Bode plot as shown in Fig. 10 and it has almost the same values (at frequency≅0 Hz, 6∼6.2 Ωcm^2) as the values obtained from the slope of VI curves in Fig. 7 and Fig. 8 in which 5∼7 Ωcm^2 were obtained. For feeding rates of 6 and 8 sccm, all points in the frequency arc in both impedance spectra overlap each other along the slope of 45°. At 10 sccm, the arc shows a small variation at low and at high frequency. Again, the differences in impedance $|Z|$ can clearly be noted in Fig. 10 where the impedance has a slightly higher value at a lower frequency, f≅0 Hz and a higher frequency, f≥25 kHz for 10 sccm. This is perhaps because, as stated previously, mass transport was limited on the membrane and at the cathode surface at f≅0 Hz. In fact, nearly 6.2 Ωcm^2 impedance was found for 10 sccm compared to that of 6 Ωcm^2 for 6 and 8 sccm at the frequency f≅0 Hz, while for f≥25 kHz, there seems to have been slightly higher uncompensated contact resistance and ohmic resistance. Exact reasons are not understood at this stage. More data may be collected and gathered in the future study to further examine the EIS dynamic response in this regard.

Conclusions

For the first time, a micro PEMFC with SU-8 flow field plates was developed and tested with operational

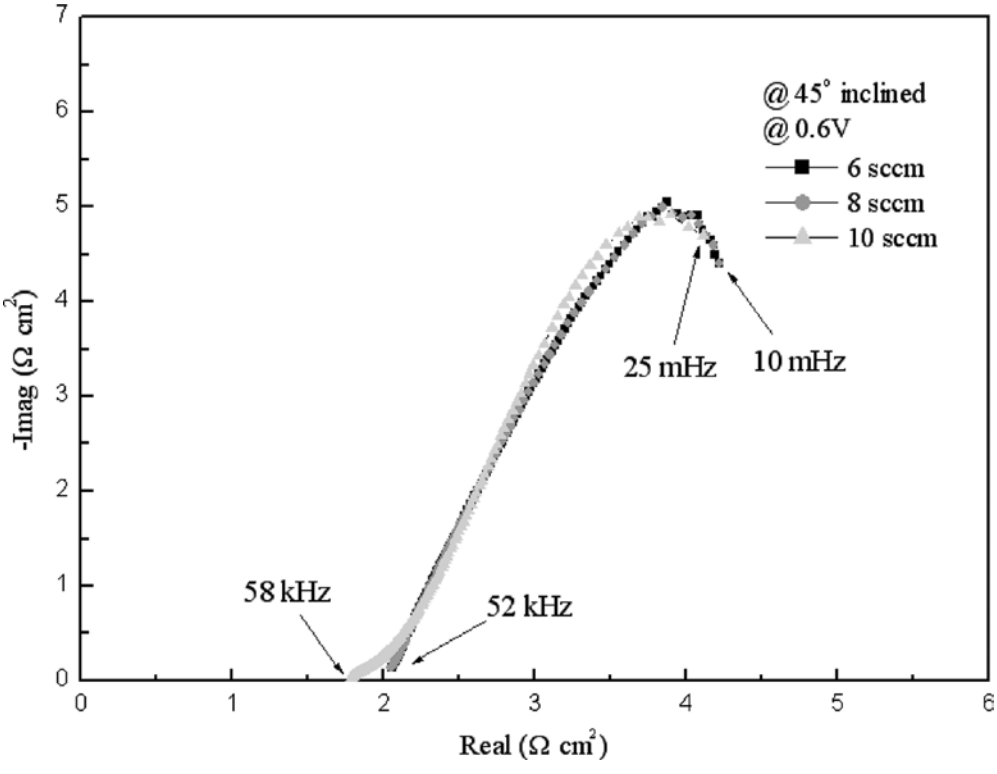

Fig. 9 Measured AC impedance spectra for a micro PEMFC at 0.6 V for 45°-inclined cathode surface

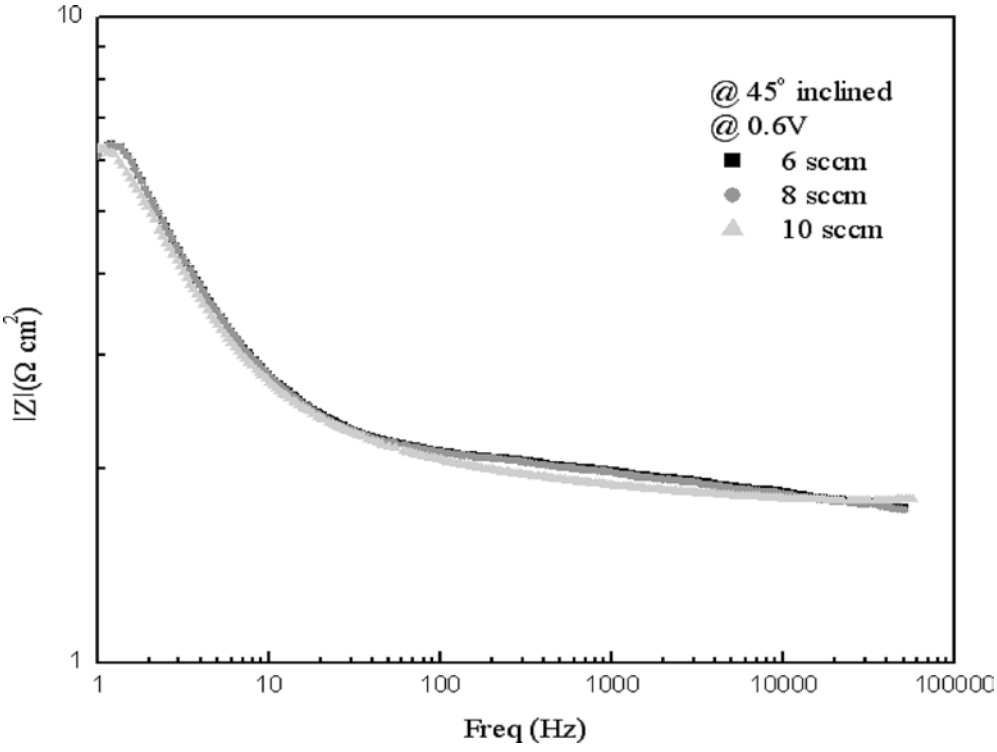

Fig. 10 The Bode plot at 0.6 V for 45°-inclined cathode surface

parameters. An in-house-made single micro PEMFC with a cross section of 5 cm^2 and thickness of about 750 μm was used for the study. The operational parameters included the anode reactant gas feeding rate as well as cathode reactant gas feeding condition (airbreathing/forced air), and the orientation of the cathode plate. The major results can be summarized as follows:

-1. A low-cost and high-mass production small flat single fuel cell with an acceptable power density of about 30 mW/cm^2 at 0.35 V has been fabricated and tested.
-2. The cell polarization curves showed only two stages. It seems that no electrochemical activation processes took place. It is perhaps due to the miniaturized nature of the micro PEMFC.
-3. Performance tests were conducted with different H_2 feeding rates at the anode with air fed through free convection mode. Among those feeding rates studied, an optimum H_2 feeding rate was found. For forced airflows, the results in cell performance show their superiority to those of airbreathing, as does the conventional fuel cell.
-4. The orientation of the cathode surface, unlike in conventional fuel cells, seems to have little influence on cell performance. In spite of this, a 45° inclined surface/or plate would surprisingly have a negligibly higher value compared to those of vertical and horizontal placements.
-5. EIS data were obtained for one typical case for the H_2 feed rates at 0.6 V. It was found that the impedance changed little for three different feeding rates of H_2 gas with the 45°-inclined cathode surface. At low and high frequencies, minor differences were still found and the reasons why were briefly discussed.

Acknowledgements This work was performed in University Microsystem Laboratory, National Sun Yat-Sen University. Financial support form National Science Council (NSC) under grant numbers NSC 92-2218-E110-014 and NSC 92-2218-E110-015 is gratefully acknowledged.

References

1. Meyers JP, Maynard HL (2002) J Power Sources 109:76
2. Chang H, Kim JR, Cho JH, Kim HK, Chai KH (2002) Solid State Ionics 148:601
3. Kordesch K, Simader G (1996) Fuel cells and applications, VCH, Weinheim, p73
4. O'Hayre R, Lee SJ, Cha SW, Prinz FB (2002) J Power Sources 109:483
5. Hsieh SS, Kuo JK, Hwang CF, Tsai HH, (2004) Microsys Technol 10:121
6. Hwang JJ, Hwang HS (2002)J Power Sources 114:24
7. Li PW, Zhong T, Wang QM, Schaofer L, Chyu MK (2003) J Power Sources 114:63
8. Fatikow S, Rembold U (1997) Microsystem technology and microrobotics. Springer, Berlin Heidelberg New York